

# Photophysical and Theoretical Investigations on Fullerene/Phthalocyanine Supramolecular Complexes

Anamika Ray,<sup>†</sup> Dibakar Goswami,<sup>‡</sup> Subrata Chattopadhyay,<sup>‡</sup> and Sumanta Bhattacharya<sup>\*,†</sup>

Department of Chemistry, The University of Burdwan, Golapbag, Burdwan - 713 104, India, and Bio-Organic Division, Bhabha Atomic Research Centre, Trombay, Mumbai - 400 085, India

Received: August 9, 2008; Revised Manuscript Received: September 1, 2008

The present paper reports the photophysical aspects of a very interesting and unique host–guest interaction between fullerene and phthalocyanines, viz., free base phthalocyanine (H<sub>2</sub>-Pc) and zinc-phthalocyanine (Zn-Pc), in toluene medium. Ground state electronic interaction between these two supramolecules has been evidenced from the observation of well-defined charge transfer (CT) absorption bands in the visible region. Vertical ionization potentials of the phthalocyanines have been determined utilizing CT transition energy. Magnitude of degrees of CT reveals that, in the ground state, 2–4% CT takes place. Binding constants (*K*) for the fullerene/phthalocyanine complexes were determined from the fluorescence quenching experiment. Large *K* values in the ranges  $\sim 4.7 \times 10^4$  to  $7.3 \times 10^4$  and  $2.3 \times 10^4$  to  $2.5 \times 10^4$  dm<sup>3</sup>·mol<sup>-1</sup> were obtained for the 1:1 fullerene complexes of Zn and H<sub>2</sub>-Pc, respectively. Values of *K* suggest that both H<sub>2</sub>- and Zn-Pc could not serve as an efficient discriminators between C<sub>60</sub> and C<sub>70</sub>. Theoretical calculations as well as <sup>13</sup>C NMR studies establish that the orientation of C<sub>70</sub> toward phthalocyanine is favored in end-on orientation, which proves that interaction between fullerenes and phthalocyanines were governed by the electrostatic mechanism rather than dispersive forces associated with  $\pi$ – $\pi$  interaction.

## 1. Introduction

Noncovalent interactions play crucial role in designing supramolecular materials using simple molecular building blocks by means of self-assembly and self-organization techniques.<sup>1–3</sup> Phthalocyanines<sup>4</sup> (Pcs) have been employed extensively as subunits for the construction of functional materials. As a result of their self-organizing abilities to form Langmuir–Blodgett multilayers<sup>5</sup> and aggregation in solution,<sup>6</sup> they efficiently exhibit special optical and electronic properties. As structural analogues of porphyrins with unusual linear and nonlinear optical properties, phthalocyanines are 18  $\pi$ -electron aromatic macrocycles perfectly suited for their energy conversion systems.<sup>7</sup> Pcs exhibit very high extinction coefficient around 700 nm, rich redox chemistry and can be self-assembled via  $\pi$ – $\pi$  stacking interactions.<sup>8</sup>

On the other hand, fullerenes are also employed as suitable building blocks for the development of multicomponent systems because of their three-dimensional structure, relatively low reduction potentials and strong electron acceptor properties.<sup>9</sup> Therefore, much attention has been paid to the study of fullerenes and phthalocyanines. In recent past, several examples of molecular<sup>10–12</sup> and supramolecular<sup>13,14</sup> architectures bearing Pc (or related compounds) and C<sub>60</sub> units have synthesized and studied.

Supramolecular C<sub>60</sub> and Pc dimers have self-assembled via hydrogen bonding between complementary recognition motifs.<sup>15</sup> In particular, Torres et al. recently reported efficient charge separation of a cytidine–guanosine fullerene/Pc dyad.<sup>16</sup> As a result of this, combination of fullerene with phthalocyanine can be a promising candidate for possible application in optoelec-

**TABLE 1: Absorption Maxima and Transition Energies for CT Complexes of H<sub>2</sub>-Pc, Degrees of Charge Transfer ( $\alpha$ ), and Experimentally Determined Vertical Ionization Potential ( $I_D^v$ ) of H<sub>2</sub>-Pc**

| electron acceptor   | $\lambda_{\max}$ , nm | $h\nu_{CT}$ , eV | $\alpha$ , % | $I_D^v$ , eV |
|---------------------|-----------------------|------------------|--------------|--------------|
| C <sub>60</sub>     | 785                   | 1.58             | 2.03         |              |
| C <sub>70</sub>     | 694                   | 1.79             | 1.42         |              |
| TCNQ                | 727                   | 1.70             | 0.91         | 7.28         |
| TCNE                | 410                   | 1.69             | 3.62         |              |
| <i>p</i> -chloranil | 431                   | 3.02             |              |              |

tronics and as organic solar cells.<sup>17</sup> Because fullerenes have good electron accepting capability, it is possible that they may interact with electron donors like Pc through charge transfer (CT) interactions. Guldi et al.<sup>18</sup> have reported similar sort of CT interaction in their designed fullerene/phthalocyanine ensembles. It was also observed that fullerene doped Zn-Pc composites generated photoconductivity due to the formation of an intermolecular CT complex between C<sub>60</sub> and Zn-Pc.<sup>19</sup> Other than the above studies, the combination of Pc and fullerenes via immobilization of the dyes in a suitable host matrix also gaining current impetus.<sup>20,21</sup> However, all of these studies are based upon covalently linked fullerene/Pc systems. As a consequence of our increasing interest in the characterization of noncovalent organization features and photophysical properties of fullerenes and related compounds,<sup>22,23</sup> we report here an interesting binding motif of H<sub>2</sub>-Pc and Zn-Pc (Figure 1) toward C<sub>60</sub> and C<sub>70</sub> in toluene medium. These two class of novel materials assemble in solution forming stable noncovalent CT complexes with high value of binding constants (*K*).

## 2. Materials and Methods

C<sub>60</sub> and C<sub>70</sub> were purchased from Aldrich, USA. Both H<sub>2</sub>- and Zn-Pc (Figure 1) were obtained from Sigma-Aldrich,

\* Corresponding author. Fax: +91-342-2530452. E-mail: sum\_9974@rediffmail.com.

<sup>†</sup> The University of Burdwan.

<sup>‡</sup> Bhabha Atomic Research Centre.

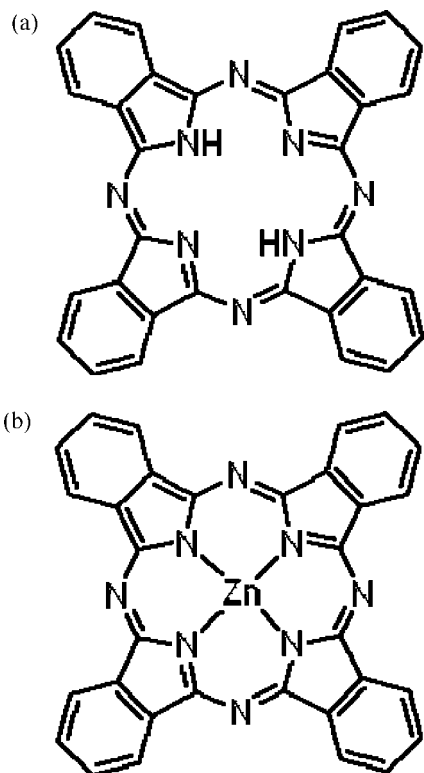


**Figure 1.** Structures of (a) H<sub>2</sub>- and (b) Zn-Pc.

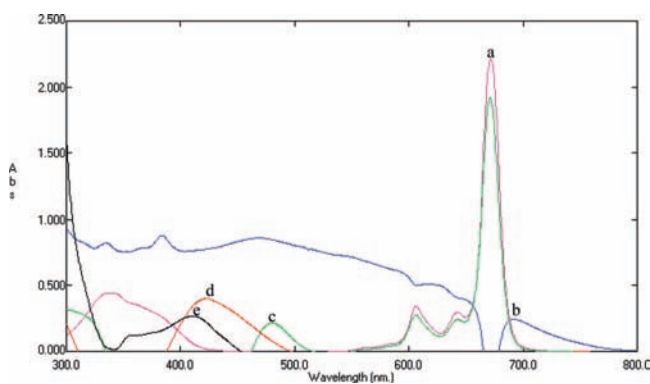


**Figure 2.** UV-vis absorption spectra of (a) only Zn-Pc and its CT complexes with (b) C<sub>70</sub>, (c) TCNQ, (d) TCNE and (e) *p*-chloranil in toluene medium.

**TABLE 2: Absorption Maxima and Transition Energies for CT Complexes of H<sub>2</sub>-Pc, Degrees of Charge Transfer ( $\alpha$ ), and Experimentally Determined Vertical Ionization Potential ( $I_D^v$ ) of Zn-Pc**

| electron acceptor   | $\lambda_{\max}$ , nm | $h\nu_{CT}$ , eV | $\alpha$ , % | $I_D^v$ , eV |
|---------------------|-----------------------|------------------|--------------|--------------|
| C <sub>60</sub>     | 730                   | 1.70             | 2.95         |              |
| C <sub>70</sub>     | 702                   | 1.77             | 2.43         |              |
| TCNQ                | 482                   | 2.57             | 2.02         | 7.77         |
| TCNE                | 430                   | 3.05             | 4.22         |              |
| <i>p</i> -chloranil | 407                   | 2.90             | 1.20         |              |

USA. The electron acceptors, viz., *p*-chloranil and 2,3,5,6-tetracyanoquinodimethane (TCNQ) were collected from Sigma-Aldrich, USA. Tetracyanoethylene (TCNE) was collected from Aldrich, USA. The solvent toluene was of UV spectroscopic grade and was collected from Merck, Germany. All UV-vis spectral measurements were recorded on a UV 1601 PC model Shimadzu spectrophotometer fitted with a Peltier controlled thermo bath. Steady state fluorescence quenching measurements were performed in a F-4500 Hitachi

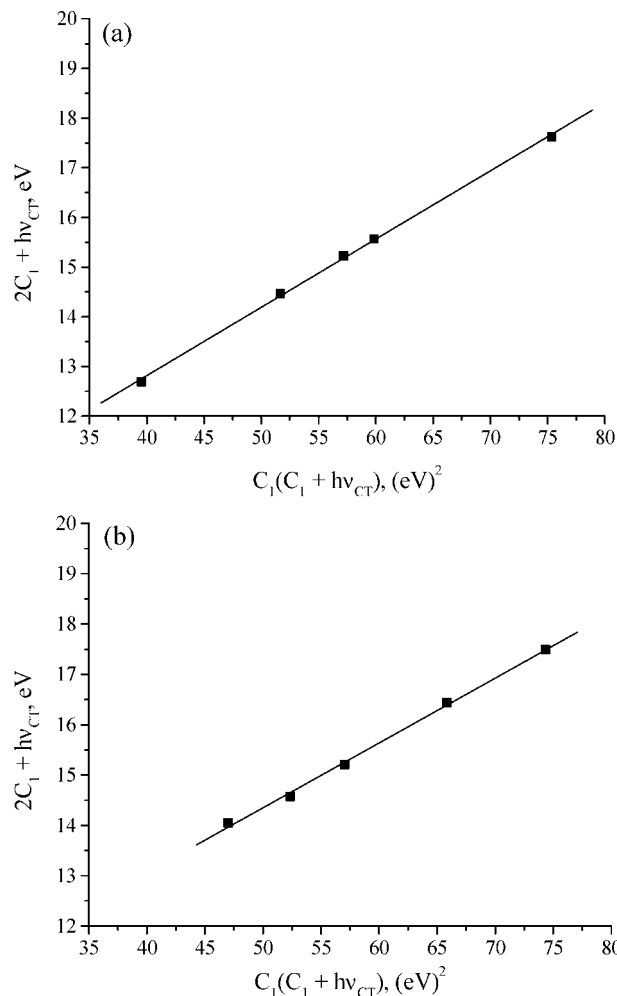


**Figure 3.** Plot of  $2C_1 + h\nu_{CT}$  vs  $C_1(C_1 + h\nu_{CT})$  for determination of  $E_A^v$  of (a) H<sub>2</sub>- and (b) Zn-Pc.

spectrofluorimeter. <sup>13</sup>C NMR measurements were recorded in a Bruker, USA, 270 MHz NMR spectrometer. Ab initio and density functional theoretical calculations (DFT) were done using SPARTAN '06 Windows software.

### 3. Results and Discussion

**3.1. Observation of CT Bands.** Evidence in favor of interactions between fullerenes and phthalocyanines first comes from UV-vis spectroscopic measurements. Addition of fullerene solution to a toluene solution of both H<sub>2</sub>- and Zn-Pc causes appearance of additional absorption peak in the visible region. This observation is a good fingerprint in favor of complexation between fullerenes and Pcs, leading us to postulate electronic interactions between these two chromophores, in the ground state. Identification of the CT spectra in the UV-vis spectroscopic experiment of fullerene/phthalocyanine complex is quite interesting as Torres et al. did not get any significant ground state electronic interactions in their designed supramolecular Pc/C<sub>60</sub> dyad.<sup>24</sup> Figure 2 shows the electronic absorption spectra of Zn-Pc and mixtures containing Zn-Pc + C<sub>60</sub>, Zn-Pc + C<sub>70</sub>, Zn-Pc + TCNQ, Zn-Pc + TCNE and Zn-Pc + *p*-chloranil, in toluene medium. Figure 1S (Supporting Information) shows the electronic absorption spectra of remaining mixtures containing H<sub>2</sub>-Pc with C<sub>60</sub>, C<sub>70</sub>, TCNQ, TCNE and *p*-chloranil in toluene medium. The notable feature of the present investigations is that the complexes of H<sub>2</sub>- and Zn-Pc with various electron

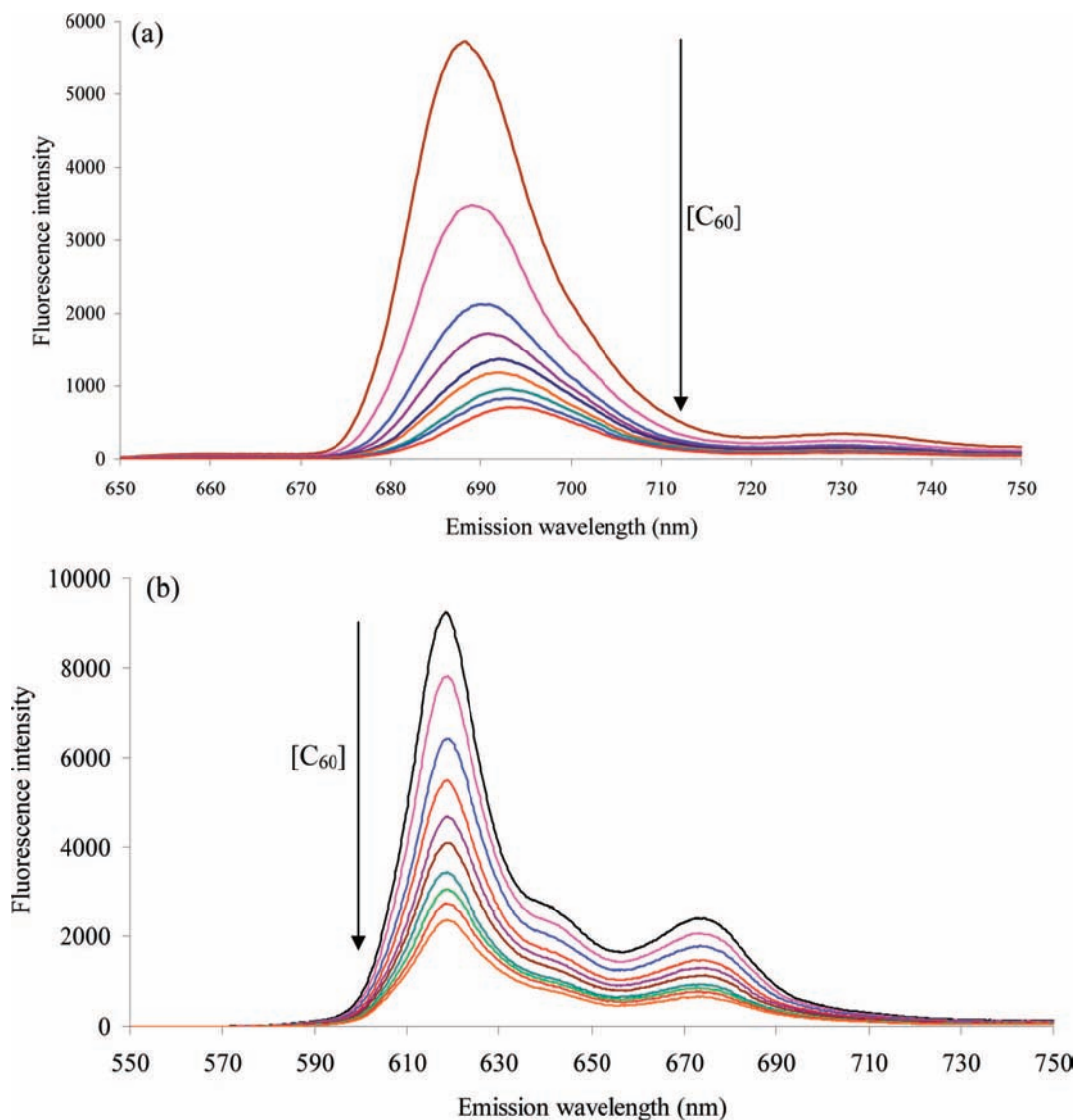


**Figure 4.** Fluorescence spectral variation of  $\text{H}_2\text{-Pc}$  ( $1.35 \times 10^{-5} \text{ mol}\cdot\text{dm}^{-3}$ ) in the presence of (a)  $\text{C}_{60}$ . The concentrations of  $\text{C}_{60}$  from top to bottom in the arrow (indicated in the figure) are as follows:  $0$ ,  $8.277 \times 10^{-6}$ ,  $16.55 \times 10^{-6}$ ,  $20.69 \times 10^{-6}$ ,  $24.83 \times 10^{-6}$ ,  $28.97 \times 10^{-6}$ ,  $33.11 \times 10^{-6}$ ,  $37.25 \times 10^{-6}$  and  $41.38 \times 10^{-6} \text{ mol}\cdot\text{dm}^{-3}$ . (b)  $\text{Zn-Pc}$  ( $6.11 \times 10^{-6} \text{ mol}\cdot\text{dm}^{-3}$ ) in the presence of  $\text{C}_{60}$ . The concentrations of  $\text{C}_{60}$  from top to bottom in the arrow (indicated in the figure) are as follows:  $0$ ,  $4.72 \times 10^{-6}$ ,  $9.45 \times 10^{-6}$ ,  $1.42 \times 10^{-5}$ ,  $1.89 \times 10^{-5}$ ,  $2.36 \times 10^{-5}$ ,  $2.83 \times 10^{-5}$ ,  $3.31 \times 10^{-5}$ ,  $3.78 \times 10^{-5}$  and  $4.25 \times 10^{-5} \text{ mol}\cdot\text{dm}^{-3}$ .

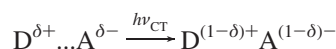
**TABLE 3: Binding Constants ( $K$ ,  $\text{dm}^3\cdot\text{mol}^{-1}$ ) and Theoretically Determined  $\Delta H_f^\circ$  Values for the Fullerene ( $\text{C}_{60}$  and  $\text{C}_{70}$ ) Complexes of  $\text{H}_2$ - and  $\text{Zn-Pc}$**

| system                               | $K$ , $\text{dm}^3\cdot\text{mol}^{-1}$ | $\Delta H_f^\circ$ , $\text{kcal}\cdot\text{mol}^{-1}$ |                   | $\Delta S_f^\circ$ , $\text{cal}\cdot\text{K}^{-1}\cdot\text{mol}^{-1}$ |                   |
|--------------------------------------|---|--|-------------------|---|-------------------|
|                                      |   | HF   | DFT               | HF  | DFT               |
| $\text{C}_{60}/\text{H}_2\text{-Pc}$ | 47440                                   | -0.052   | -0.8050           | -23.30  | -24.24            |
| $\text{C}_{70}/\text{H}_2\text{-Pc}$ | 73530                                   | -0.993 (side on)                                       | -41.151 (side on) | -25.75 (side on)  | -160.50 (side on) |
|                                      |   | -0.974 (end on)  | -41.367 (end on)  | -25.68 (end on)   | -161.23 (end on)  |
| $\text{C}_{60}/\text{Zn-Pc}$         | 23500                                   | -5.478   | -4.479            | -1.75   | -5.10             |
| $\text{C}_{70}/\text{Zn-Pc}$         | 25690                                   | -5.031 (side on)                                       | -35.32 (side on)  | -3.42 (side on)   | -138.82 (side on) |
|                                      |   | -5.025 (end on)  | -35.274 (end on)  | -3.44 (end on)  | -138.67 (end on)  |

acceptors do not exhibit any sort of typical spectral characteristics of parent uncomplexed phthalocyanines. To obtain the CT bands, spectra of above solutions (in toluene medium) were recorded against the pristine phthalocyanine (donor) solution as reference to cancel out the donor's absorbance. The solvent toluene does not absorb in the visible region. It is a common experience that to detect CT absorption bands in solution, the donor (in present case phthalocyanine) concentration must be

made very high compared to that of the acceptor. In our present case,  $[\text{acceptor}] \sim 10^{-5} \text{ mol}\cdot\text{dm}^{-3}$  and  $[\text{phthalocyanine}] \sim 10^{-4} \text{ mol}\cdot\text{dm}^{-3}$  in the mixture. The CT absorption spectra were analyzed by fitting to the Gaussian function  $y = y_0 + [A/(w\sqrt{\pi/2})] \exp[-2(x - x_c)^2/w^2]$ , where  $x$  and  $y$  denote wavelength and absorbance, respectively. The wavelengths at these new absorption maxima ( $\lambda_{\text{max}} = x_c$ ) and the corresponding transition energies ( $h\nu$ ) are summarized in Table 1.

**3.2. Determination of Vertical Ionization Potential ( $I_D^V$ ) of  $H_2$ - and  $Zn$ -Pc.** For complexes with neutral ground state, a CT band corresponds to a transfer of an electron from a donor to an acceptor molecule with the absorption of a quantum:



The relationship between the energy ( $h\nu_{CT}$ ) of the lowest energy intermolecular CT band and the  $I_D^V$  of the donor for a series of complexes with a common acceptor species has been the source of much discussion. According to Mulliken's theory<sup>25</sup> the ground state of the complex is a resonance hybrid of a "no-bond" state ( $D \dots A$ ) and a dative state ( $D^+A^-$ ) with the former predominating; the excited state is a resonance hybrid of the same two structures with the dative one predominating. CT transition energies of these complexes are related to the vertical ionization potentials ( $I_D^V$ ) of the donors by the relation,

$$h\nu_{CT} = [I_D^V / (I_D^V - C_1)] \quad (1)$$

Here

$$C_1 = E_A^V + G_0 + G_1 \quad (2)$$

where  $E_A^V$  is the vertical electron affinity of the acceptor;  $G_0$ , sum of several energy terms (like dipole-dipole, van der Waals interaction, etc.) in the "no-bond" state; and  $G_1$ , sum of a number of energy terms in the "dative" state. In most cases  $G_0$  is small

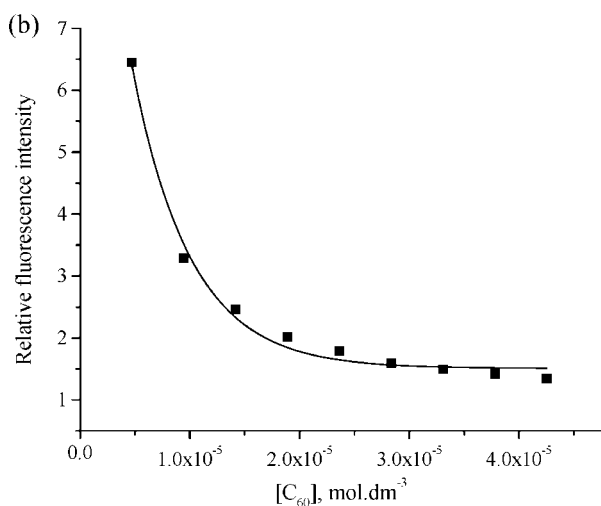
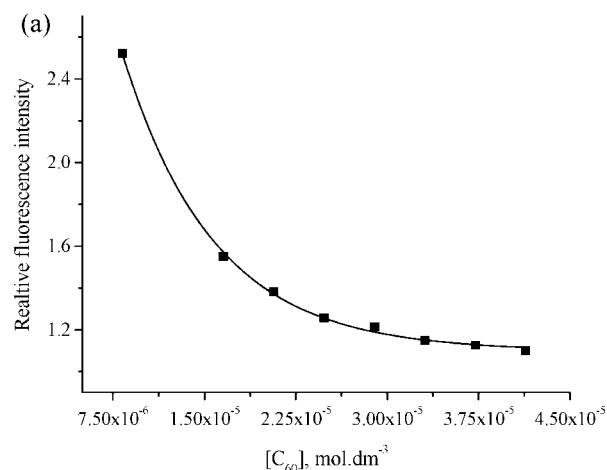


**Figure 5.** Relative fluorescence intensity vs concentration plots for (a)  $C_{60}/H_2$ -Pc and (b)  $C_{60}/Zn$ -Pc systems.

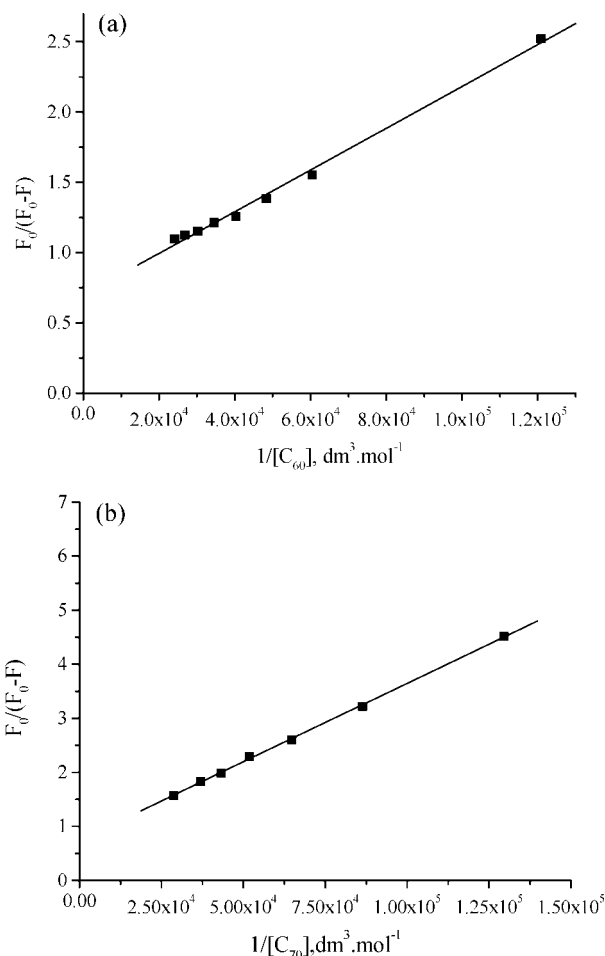


**Figure 6.** BH fluorescence plots of (a)  $C_{60}/H_2$ -Pc and (b)  $C_{70}/Zn$ -Pc systems in toluene medium.

and can be neglected whereas  $G_1$  is largely the electrostatic energy of attraction between  $D^+$  and  $A^-$ . The term  $C_2$  in eq 1 is related to the resonance energy of interaction between the "no-bond" and "dative" forms in the ground and excited states and for a given acceptor it may be supposed to be constant.<sup>25</sup> A rearrangement of eq 1 yields

$$2C_1 + h\nu_{CT} = (1/I_D^V)C_1(C_1 + h\nu_{CT}) + \{(C_2/I_D^V) + I_D^V\} \quad (3)$$

The vertical electron affinities of  $C_{60}$ ,  $C_{70}$ , *p*-chloranil, TCNQ and DDQ were collected from literature.<sup>26-30</sup> Neglecting  $G_0$  and taking the typical D-A distance in  $\pi$ -type CT complexes to be 3.5 Å, the major part of  $G_1$  is estimated to be  $e^2/4\pi\epsilon_0 r = 4.13$  eV. Using these values,  $C_1$  is obtained from eq 2 for each of the acceptors. A plot of  $2C_1 + h\nu_{CT}$  versus  $C_1(C_1 + h\nu_{CT})$  for a given donor and various electron acceptors yields a slope of  $1/I_D^V$  from which the values of  $1/I_D^V$  have been obtained for  $H_2$ - and  $Zn$ -Pc. Results are given in Table 2. The following linear regressions have been obtained with the present data:

$$H_2\text{-Pc: } 2C_1 + h\nu_{CT} = (0.1374 \pm 0.0024)C_1(C_1 + h\nu_{CT}) + (7.3197 \pm 0.1394); \quad \text{correlation coefficient} = 0.99 \quad (4a)$$

$$Zn\text{-Pc: } 2C_1 + h\nu_{CT} = (0.1286 \pm 0.0035)C_1(C_1 + h\nu_{CT}) + (7.9167 \pm 0.1286); \quad \text{correlation coefficient} = 0.99 \quad (4b)$$

The above plots are demonstrated in Figure 3.

**TABLE 4: Comparison of Five Highest Occupied and Five Lowest Unoccupied Molecular Orbital Levels of H<sub>2</sub>-Pc, Zn-Pc, C<sub>60</sub>, C<sub>60</sub>/H<sub>2</sub>-Pc and C<sub>60</sub>/Zn-Pc Systems Done by HF/3-21G Calculations**

| state  | energy, eV         |         |                 |                                     |                        |
|--------|--------------------|---------|-----------------|-------------------------------------|------------------------|
|        | H <sub>2</sub> -Pc | Zn-Pc   | C <sub>60</sub> | C <sub>60</sub> /H <sub>2</sub> -Pc | C <sub>60</sub> /Zn-Pc |
| HOMO-4 | -9.2815            | -9.3770 | -8.2756         | -8.1427                             | -8.1774                |
| HOMO-3 | -9.1429            | -9.1820 | -8.2756         | -8.1385                             | -8.1753                |
| HOMO-2 | -9.1002            | -9.0275 | -8.2756         | -8.1345                             | -8.1743                |
| HOMO-1 | -8.7692            | -8.7668 | -8.2755         | -8.1308                             | -8.1716                |
| HOMO   | -5.9616            | -5.5109 | -8.2755         | -5.9832                             | -5.5257                |
| LUMO   | -0.0525            | -0.2205 | -0.7690         | -0.6377                             | -0.6739                |
| LUMO+1 | -0.0537            | -0.1390 | -0.7690         | -0.6315                             | -0.6687                |
| LUMO+2 | -2.2223            | -2.3727 | -0.7690         | -0.6287                             | -0.6674                |
| LUMO+3 | -2.4904            | -2.6085 | -0.8930         | -0.0716                             | -0.2119                |
| LUMO+4 | -3.0991            | -2.8449 | -0.8930         | -0.0386                             | -0.1154                |

**3.3. Determination of Degrees of Charge Transfer ( $\alpha$ ).** A rearrangement of eq 1 gives

$$2I_D^v - hv_{CT} = (1/C_1)I_D^v(I_D^v - hv_{CT}) + \{C_1 + (C_2/C_1)\} \quad (5)$$

Utilizing the values of  $C_1$  and  $C_2$  obtained from eq 5, degrees of charge transfer ( $\alpha$ ) for the CT complexes of H<sub>2</sub>- and Zn-Pc can be calculated as follows:

$$\alpha = (C_2/2)/[(I_D^v - E_A^v + C_1)^2 + (C_2/2)] \quad (6)$$

All the values of  $\alpha$  are listed in Tables 1 and 2. The values of  $\alpha$  (calculated by using eq 6) are small and indicate that very little amount of charge transfer occurs in the ground state. Variation of  $\alpha$  with the electron affinity of the acceptors is nonlinear (Figure 2S, Supporting Information). This is quite

expected as the model we use here to determine various electronic parameters are based upon interaction of a common donor species with structurally dissimilar electron acceptors. For this reason, we have got a nonlinear variation in the plot of  $\alpha$  vs  $E_A^v$ . Following correlations have been obtained with the present data:

$$\text{H}_2\text{-Pc:} \quad \alpha = 3.885 - 147.3476E_A^v + 3595.6177(E_A^v)^2 \quad (7a)$$

$$\text{Zn-Pc:} \quad \alpha = 4.908 - 177.9027E_A^v + 3271.0439(E_A^v)^2 \quad (7b)$$

**3.4. Fluorescence Spectroscopic Studies.** As far as the emission spectra were concerned, it must be pointed out that in

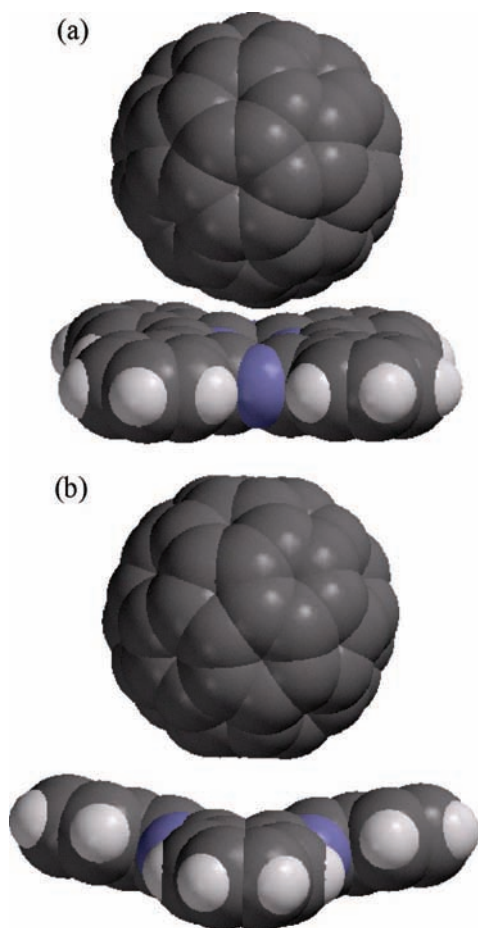


**Figure 7.** Space filling models of the C<sub>60</sub> complexes of (a) H<sub>2</sub>- and (b) Zn-Pc obtained at HF/3-21G calculations.

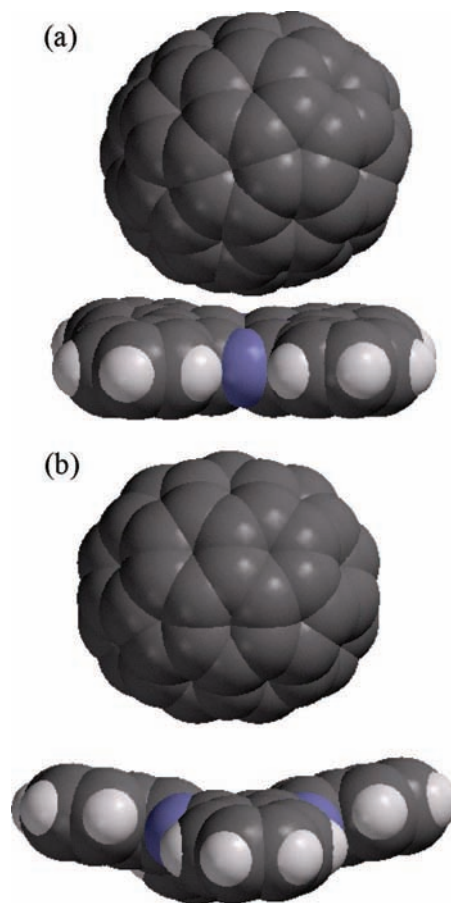


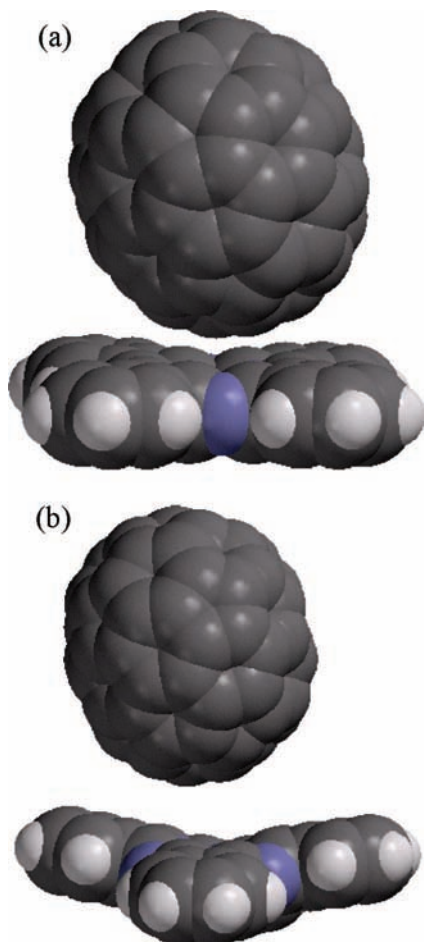
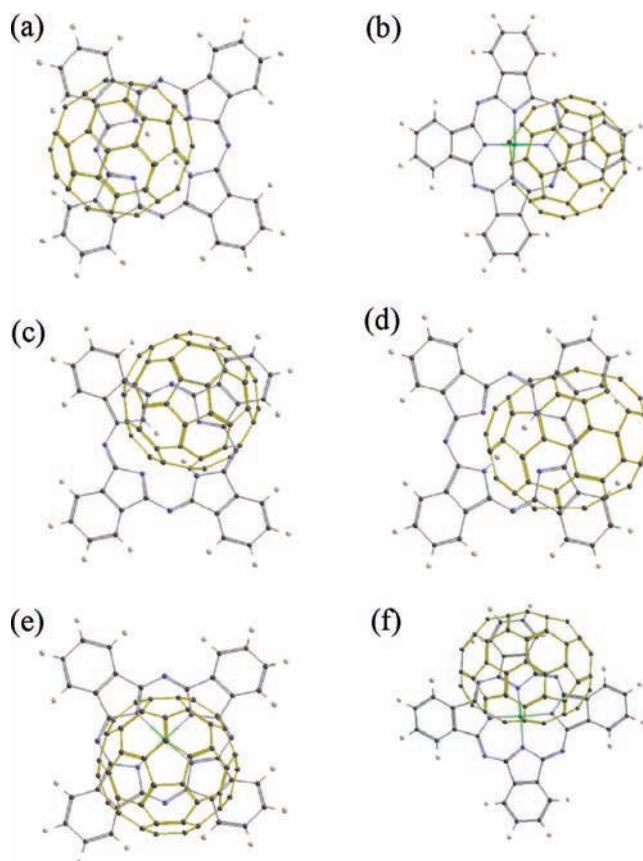
**Figure 8.** Space filling models of the C<sub>70</sub> complexes of (a) H<sub>2</sub>- and (b) Zn-Pc in side-on orientation of C<sub>70</sub> obtained at HF/3-21G calculations.

**TABLE 5: Comparison of Five Highest Occupied and Five Lowest Unoccupied Molecular Orbital Levels of  $C_{70}$ ,  $C_{70}/H_2\text{-Pc}$  and  $C_{70}/Zn\text{-Pc}$  Systems Done by HF/3-21G Calculations in Different Orientations of  $C_{70}$** 

| state  | energy, eV |                                 |                                  |                                |                                 |
|--------|------------|---------------------------------|----------------------------------|--------------------------------|---------------------------------|
|        | $C_{70}$   | $C_{70}/H_2\text{-Pc}$ (end-on) | $C_{70}/H_2\text{-Pc}$ (side-on) | $C_{70}/Zn\text{-Pc}$ (end-on) | $C_{70}/Zn\text{-Pc}$ (side-on) |
| HOMO-4 | -8.8901    | -8.2693                         | -8.2627                          | -8.3211                        | -8.2956                         |
| HOMO-3 | -8.3859    | -7.8615                         | -7.8597                          | -7.9158                        | -7.8964                         |
| HOMO-2 | -7.9840    | -7.8609                         | -7.8593                          | -7.9156                        | -7.8949                         |
| HOMO-1 | -7.9840    | -7.7945                         | -7.7935                          | -7.8500                        | -7.8298                         |
| HOMO   | -7.9169    | -5.9882                         | -5.9858                          | -5.5276                        | -5.5274                         |
| LUMO   | -0.9531    | -0.8279                         | -0.8291                          | -0.8840                        | -0.8661                         |
| LUMO+1 | -0.9531    | -0.8262                         | -0.8283                          | -0.8832                        | -0.8659                         |
| LUMO+2 | -0.7898    | -0.6684                         | -0.6630                          | -0.7216                        | -0.6971                         |
| LUMO+3 | -0.1814    | -0.0762                         | -0.0739                          | -0.2157                        | -0.2146                         |
| LUMO+4 | -0.4724    | -0.0625                         | -0.0583                          | -0.1212                        | -0.1193                         |

our present investigations fluorescence experiments could be reliably done due to one very favorable circumstance. The large molar extinction coefficients of  $H_2\text{-Pc}$  and  $Zn\text{-Pc}$  with respect to the fullerenes in the visible UV-vis spectral region allowed us to preferentially excite the Pcs, although the Pc concentration was much lower than those of the fullerenes. It was observed that fluorescence of  $Zn\text{-Pc}$  at 679, upon excitation at 336 nm (i.e., Soret-absorption band), was diminished gradually by the addition of varying concentration of  $C_{60}$  or  $C_{70}$  in toluene medium. The fluorescence spectral changes of  $H_2\text{-Pc}$  and  $Zn\text{-Pc}$  upon addition of  $C_{60}$  solution are shown in Figure 4. The emission peak of the phthalocyanines under consideration corroborate fairly well with the reported literature value of

various other phthalocyanines<sup>31,32</sup> It is already reported that light induced energy or electron transfer reactions took place in self-assembled supramolecular zinc porphyrin/zinc phthalocyanine and fullerene bearing donor-acceptor systems.<sup>33</sup> Competing between the energy and electron transfer process is an universal phenomenon in a donor-fullerene molecular complex, solvent dependent photophysical behavior is a typical phenomena of the most supramolecular fullerene systems studied to date.<sup>34-36</sup> Usually, energy transfer dominates the photophysical behavior in nonpolar solvent in deactivating the photoexcited chromophore  $*H_2\text{-Pc}$  and  $*Zn\text{-Pc}$ . In present investigations, therefore, the quenching phenomenon can be ascribed to the photoinduced energy transfer from phthalocyanines to fullerenes in the fullerene/ $H_2\text{-Pc}$  and fullerene/ $Zn\text{-Pc}$  supramolecular

**Figure 9.** Space filling models of the  $C_{70}$  complexes of (a)  $H_2\text{-Pc}$  and (b)  $Zn\text{-Pc}$  in end-on orientation of  $C_{70}$  obtained at HF/3-21G calculations.**Figure 10.** Stereoscopic structures of (a)  $C_{60}/H_2\text{-Pc}$ , (b)  $C_{60}/Zn\text{-Pc}$ , (c)  $C_{70}/H_2\text{-Pc}$  (end-on orientation of  $C_{70}$ ), (d)  $C_{70}/H_2\text{-Pc}$  (side-on orientation of  $C_{70}$ ), (e)  $C_{70}/Zn\text{-Pc}$  (end-on orientation of  $C_{70}$ ) and (f)  $C_{70}/Zn\text{-Pc}$  (side-on orientation of  $C_{70}$ ) complexes obtained at DFT/B3LYP/6-31G\* calculations.

**TABLE 6: Comparison of Five Highest Occupied and Five Lowest Unoccupied Molecular Orbital Levels of H<sub>2</sub>-Pc, Zn-Pc, C<sub>60</sub>, C<sub>60</sub>/H<sub>2</sub>-Pc and C<sub>60</sub>/Zn-Pc Systems Done by DFT/B3LYP/6-31G\* Calculations**

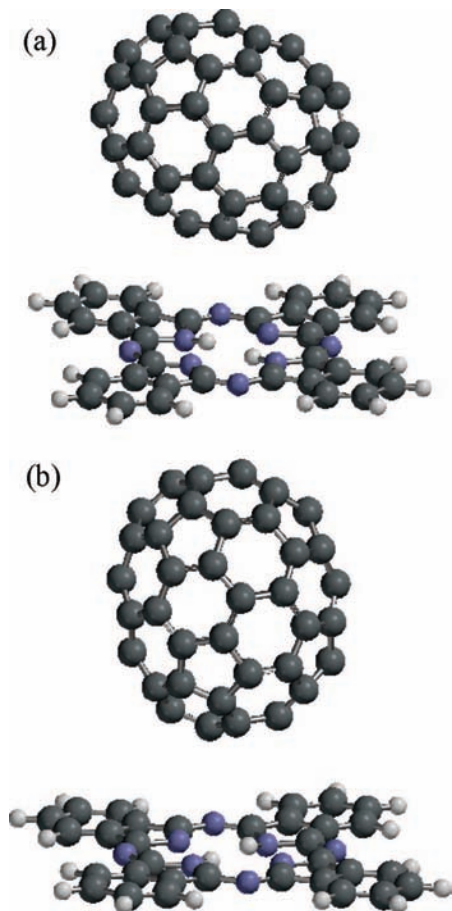
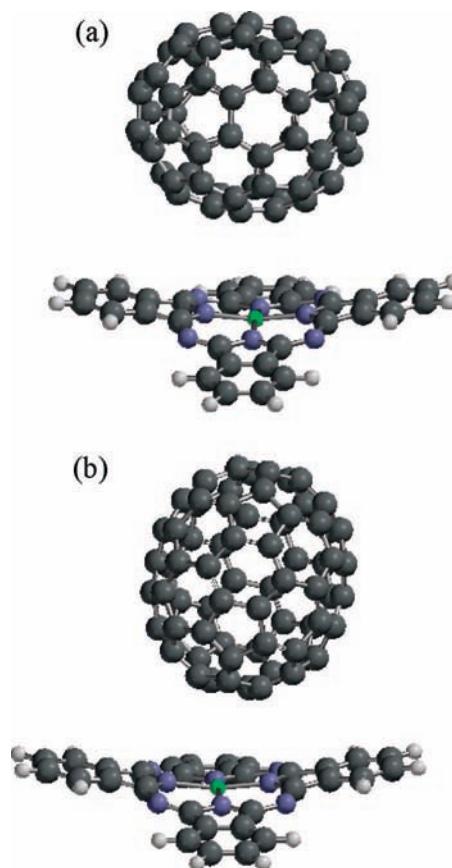
| state  | energy, eV         |         |                 |                                     |                        |
|--------|--------------------|---------|-----------------|-------------------------------------|------------------------|
|        | H <sub>2</sub> -Pc | Zn-Pc   | C <sub>60</sub> | C <sub>60</sub> /H <sub>2</sub> -Pc | C <sub>60</sub> /Zn-Pc |
| HOMO-4 | -6.9607            | -6.7709 | -6.0164         | -5.9137                             | -5.9485                |
| HOMO-3 | -6.8169            | -6.7599 | -6.0163         | -5.9127                             | -5.9480                |
| HOMO-2 | -6.5574            | -6.6296 | -6.0162         | -5.9121                             | -5.9472                |
| HOMO-1 | -6.4533            | -6.5204 | -6.0161         | -5.9106                             | -5.9466                |
| HOMO   | -5.0150            | -4.8911 | -6.0159         | -5.0312                             | -4.8907                |
| LUMO   | -2.8227            | -2.7862 | -3.1469         | -3.0458                             | -3.0798                |
| LUMO+1 | -2.8054            | -2.7597 | -3.1467         | -3.0437                             | -3.0782                |
| LUMO+2 | -1.2287            | -1.1024 | -3.1466         | -3.0427                             | -3.0776                |
| LUMO+3 | -1.0611            | -0.9372 | -1.9603         | -2.8396                             | -2.7941                |
| LUMO+4 | -0.6718            | -0.7429 | -1.9602         | -2.8215                             | -2.7607                |

complexes. The fluorescence spectral changes of H<sub>2</sub>- and Zn-Pc upon addition of C<sub>70</sub> solution are shown in Figure 3S, Supporting Information. The above titration experiments were performed at constant concentrations of both H<sub>2</sub>- and Zn-Pc. As the concentration of fullerene is increased, the emission intensity of phthalocyanine has been reduced. The spectral changes finally reach a plateau, indicating that the fluorescence quenching is induced by the complexation (Figures 5 and 4S, Supporting Information). It should be noted at this point that although Zn-Pc exhibits fluorescence quenching upon addition of C<sub>60</sub> and C<sub>70</sub>, the quenching efficiency is higher in case of H<sub>2</sub>-Pc. The binding constants (*K*) were evaluated according to a modified Benesi–Hildebrand (BH) equation<sup>37</sup> (see eq 8):

$$F_0/(F_0 - F) = (1/A) + \{(1/KA)(1/[fullerene])\} \quad (8)$$

In eq 8, *F*<sub>0</sub> and *F* are the fluorescence intensity of Pc (and/ Zn-Pc) without and with the fullerenes, respectively, and

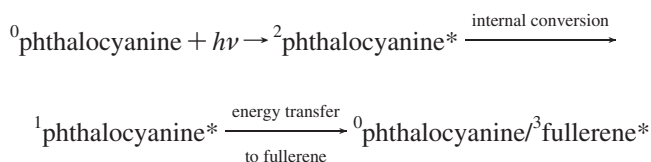
[fullerene] indicate the molar concentration of fullerene; *A* is a constant associated with the difference in the emission quantum yield of the complexed and uncomplexed phthalocyanine. By plotting *F*<sub>0</sub>/(*F*<sub>0</sub> - *F*) (relative fluorescence intensity) versus 1/[fullerene], *K* values were evaluated for various fullerene/phthalocyanine complexes (see Table 3). Two typical BH fluorescence plots of C<sub>60</sub>/H<sub>2</sub>-Pc and C<sub>70</sub>/Zn-Pc systems are shown in Figure 6. The BH plots of the complexes of C<sub>60</sub>/Zn-Pc and C<sub>70</sub>/H<sub>2</sub>-Pc systems are provided as Figure 5S, Supporting Information. In a nonpolar medium like toluene, generally, energy transfer phenomena dominates over electron transfer in deactivating the photoexcited chromophore, <sup>1</sup>H<sub>2</sub>-Pc\* and <sup>1</sup>Zn-Pc\*, formed in the final instance of the fullerene triplet excited state. This finding suggests that singlet energy transduction to give H<sub>2</sub>-Pc(/Zn-Pc)/<sup>1</sup>fullerene\* followed by generation of H<sub>2</sub>-Pc(/Zn-Pc)/<sup>3</sup>fullerene\* (by intersystem crossing) is not operative in present case. As we used the Soret absorption band as our source of excitation wavelength in fluorescence experiment, the

**Figure 11.** Ball and spoke model of C<sub>70</sub>/H<sub>2</sub>-Pc complex in (a) side-on and (b) end-on orientations.**Figure 12.** Ball and spoke model of C<sub>70</sub>/Zn-Pc complex in (a) side-on and (b) end-on orientations.

**TABLE 7: Comparison of Five Highest Occupied and Five Lowest Unoccupied Molecular Orbital Levels of C<sub>70</sub>, C<sub>70</sub>/H<sub>2</sub>-Pc and C<sub>70</sub>/Zn-Pc Systems Done by DFT/B3LYP/6-31G\* Calculations in Different Orientations of C<sub>70</sub>**

| state  | energy, eV      |  |   |                                 |                                  |
|--------|-----------------|--|---|---------------------------------|----------------------------------|
|        | C <sub>70</sub> | C <sub>70</sub> /H <sub>2</sub> -Pc (end-on) | C <sub>70</sub> /H <sub>2</sub> -Pc (side-on) | C <sub>70</sub> /Zn-Pc (end-on) | C <sub>70</sub> /Zn-Pc (side-on) |
| HOMO-4 | -6.4215         | -6.0929                                      | -6.0862                                       | -6.1305                         | -6.1198                          |
| HOMO-3 | -6.1723         | -5.8800                                      | -5.8788                                       | -5.9195                         | -5.9121                          |
| HOMO-2 | -5.9622         | -5.8319                                      | -5.8292                                       | -5.8707                         | -5.8628                          |
| HOMO-1 | -5.9148         | -5.8317                                      | -5.8284                                       | -5.8706                         | -5.8625                          |
| HOMO   | -5.9146         | -5.0341                                      | -5.0329                                       | -4.8944                         | -4.8939                          |
| LUMO   | -3.1427         | -3.0574                                      | -3.0578                                       | -3.0974                         | -3.0916                          |
| LUMO+1 | -3.1426         | -3.0572                                      | -3.0575                                       | -3.0971                         | -3.0912                          |
| LUMO+2 | -2.9799         | -2.8970                                      | -2.8923                                       | -2.9352                         | -2.9255                          |
| LUMO+3 | -2.6151         | -2.8424                                      | -2.8413                                       | -2.7979                         | -2.7972                          |
| LUMO+4 | -2.2732         | -2.8244                                      | -2.8229                                       | -2.7654                         | -2.7645                          |

second excited singlet state of the phthalocyanine, was deactivated by following mechanism:



A similar sort of experimental observations was already reported by Yin et al.<sup>38</sup> and Guldi et al.<sup>39</sup> for their particular designed supramolecule containing C<sub>60</sub>. It is interesting to note that the increase in magnitude of binding constant led to increase of the fluorescence quenching efficiency. This can be viewed in terms of the fact that the rigidity of the phthalocyanine unit brings tight fixation of C<sub>60</sub> and C<sub>70</sub> unit in phthalocyanine/fullerene host-guest complex.

**3.5. Binding Constants.** The binding constants (*K*) of fullerene/phthalocyanine complexes determined by fluorescence spectra are summarized in Table 3. It shows that H<sub>2</sub>-Pc

undergoes considerable amount of complexation with both C<sub>60</sub> and C<sub>70</sub> compared to Zn-Pc. The present trend in *K* value is somewhat unnatural as structural analogue of Zn-Pc, viz., Zn-porphyrin, always gives higher magnitude of binding constant with both C<sub>60</sub> and C<sub>70</sub><sup>40,41</sup> compared to free base porphyrin.

Another interesting aspect of the present investigations is that both H<sub>2</sub>-Pc and Zn-Pc host molecule did not exhibit any sort of selectivity toward C<sub>60</sub> or C<sub>70</sub>. The selectivities of C<sub>70</sub> over C<sub>60</sub> are found to be 1.55 and 1.10 for H<sub>2</sub>- and Zn-Pc, respectively. Although, the present selectivity ratios of phthalocyanines are comparable to that of azacalix[*m*]arene[*n*]pyridine (~1.940<sup>8</sup>), they are lower than those of calixarene diporphyrin (~4.3),<sup>42</sup> cyclic dimers of Zn-porphyrins (~25.5)<sup>43</sup> and corresponding H<sub>2</sub>-diporphyrin (~32)<sup>44</sup> complexes.

From the above results we can say that in spite of huge similarity in structure of porphyrin and phthalocyanine, remarkable decrease in selectivity of *K*<sub>C<sub>70</sub></sub>/*K*<sub>C<sub>60</sub></sub> is observed in case of later. The present selectivity ratio corroborates fairly well with the observed value for fullerene/azulene complex (viz., *K*<sub>C<sub>70</sub></sub>/

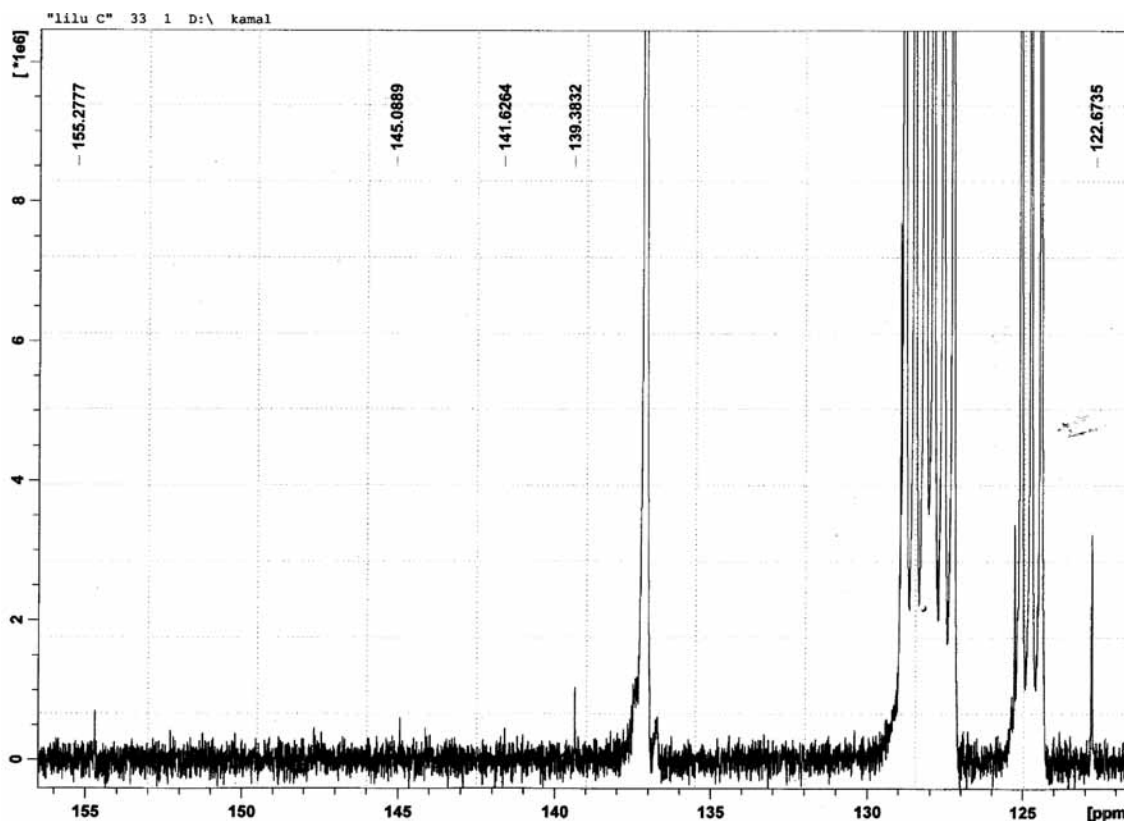


**Figure 13.** <sup>13</sup>C NMR spectrum of C<sub>70</sub>/Zn-Pc system recorded in toluene-*d*<sub>8</sub> solvent at 298 K.



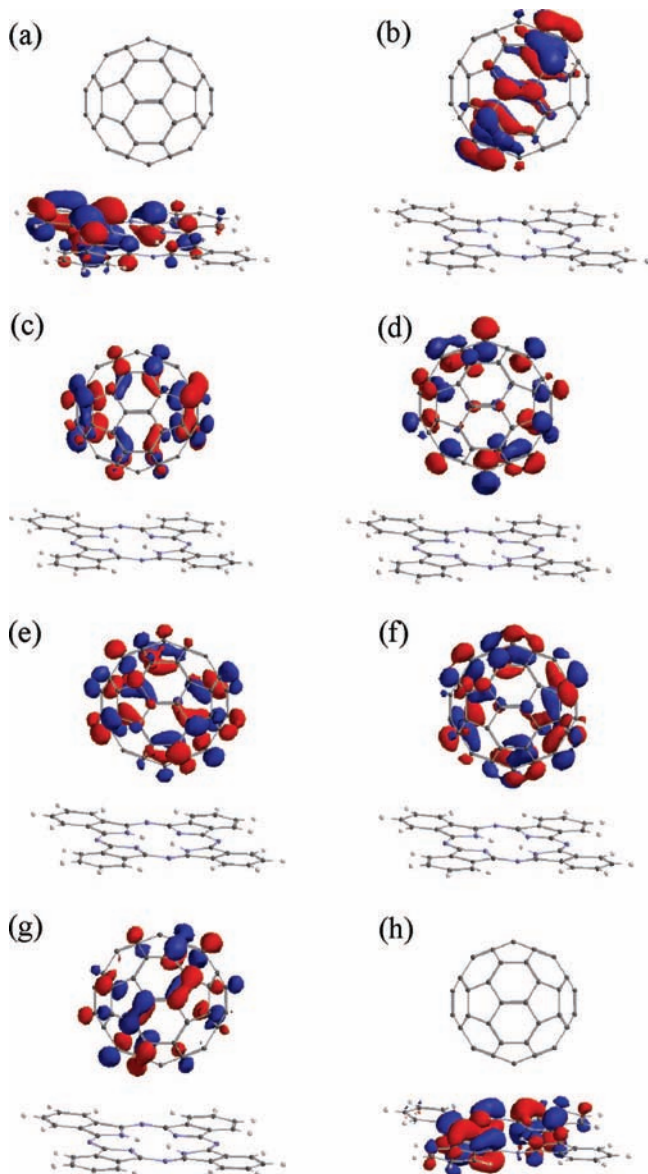


**Figure 14.** HOMOs and LUMOs of  $C_{60}/H_2\text{-Pc}$  complex at different electronic states: (a) HOMO, (b) HOMO-1, (c) HOMO-2, (d) HOMO-3, (e) LUMO, (f) LUMO+1, (g) LUMO+2 and (h) LUMO+3 done by HF/3-21G calculations.

$K_{C_{60}} = 1$ ) reported very recently by Rahman et al.<sup>45</sup> However,  $C_{70}$  produced higher value of binding constant with both  $H_2$ - and Zn-Pc compared to  $C_{60}$ . This phenomenon may be explained as follows.

It is well-known that the stability of the supramolecular complexes depends upon attractive interactions between host and guest, and on solvation of the binding partners.<sup>46</sup> In the present investigations, because the host and guest were separately solvated in solution, the desolvation of the host and guest was requisite in the association process. However, the process of desolvation is energetically an uphill task and, hence, an association takes place only when the energy gain between the host and guest interaction exceeds this unfavorable energy. From the trends in the  $K$  values of the fullerene/phthalocyanine complexes, we may infer that the extent of solvation and desolvation of the binding partners might play an important role in forming weak or strong supramolecular complexes. Haino et al.<sup>47</sup> showed that the stability of the complex increases as the solubility of fullerene in a solvent decreases, because less

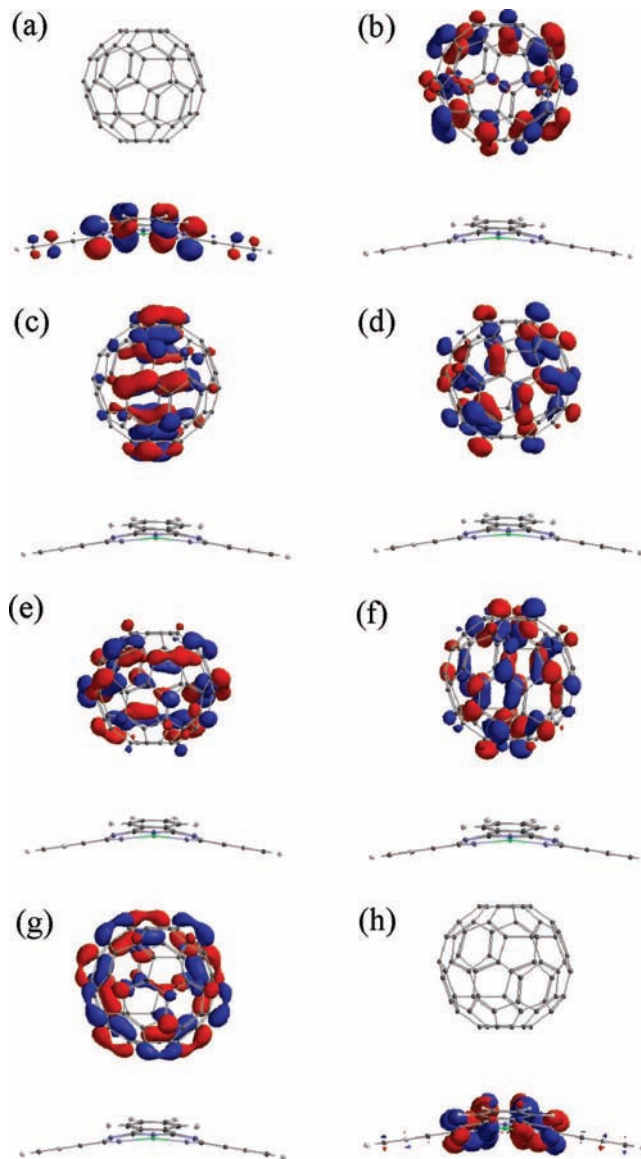


**Figure 15.** HOMOs and LUMOs of  $C_{60}/Zn\text{-Pc}$  complex at different electronic states: (a) HOMO, (b) HOMO-1, (c) HOMO-2, (d) HOMO-3, (e) LUMO, (f) LUMO+1, (g) LUMO+2 and (h) LUMO+3 done by HF/3-21G calculations.

energy is required for the desolvation of fullerene which must necessarily precede its complexation with a host molecule. This would be one of the reasons for the higher  $K$  values of the  $C_{70}$  complexes in toluene, because the solubility of  $C_{60}$  is higher in toluene (4.1 mg/mL) than that of  $C_{70}$  (2.0 mg/mL).<sup>48</sup>

**3.6. Theoretical Calculations.** To gain insight into the preferred molecular geometry and to measure the heat of formation ( $\Delta H_f^\circ$ ) values or interaction energies (IEs), a detailed conformational analysis of the individual components as well as the fullerene/phthalocyanine complexes was performed in vacuo by Hartree-Fock (HF) and density functional theory (DFT) calculations. The geometric parameters of the complexes were obtained after complete energy minimization at the HF/3-21G level of theory. For the energy classification of the optimized structures, we used the following (standard) interaction energy (IE) (i.e.,  $\Delta H_f^\circ$ ) definitions. IEs have been estimated within the supramolecular approach  $IE = E_{\text{complex}} - [E_{\text{fullerene}} + E_{\text{Pc}}]$  (where  $E_{\text{complex}}$ ,  $E_{\text{fullerene}}$  and  $E_{\text{Pc}}$ , are the energy of fullerene/Pc complex, uncomplexed fullerene and free Pc, respectively) to determine the total strength of the various

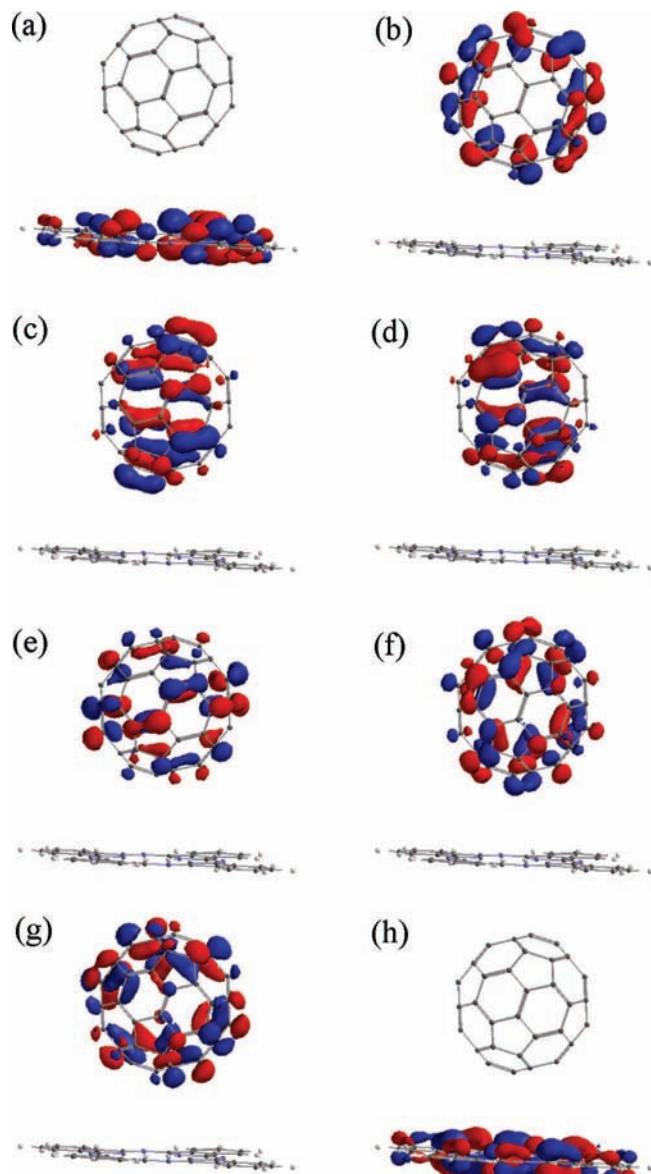


**Figure 16.** HOMOs and LUMOs of the  $C_{60}/H_2\text{-Pc}$  complex at different electronic states: (a) HOMO, (b) HOMO-1, (c) HOMO-2, (d) HOMO-3, (e) LUMO, (f) LUMO+1, (g) LUMO+2 and (h) LUMO+3 done by DFT/B3LYP/6-31G\* calculations.

interaction patterns between the fullerenes ( $C_{60}$  and  $C_{70}$ ) and the receptor, e.g.,  $H_2\text{-}$  and  $Zn\text{-Pc}$ .

Comparing the relative stability in terms of  $\Delta H_f^\circ$  as listed in Table 3, it was revealed that enthalpy differences were very small between the  $C_{70}$  complexes of same receptor molecule, i.e.,  $H_2\text{-}$  and  $Zn\text{-Pc}$  in different orientations of  $C_{70}$ , which proved that the  $\Delta H_f^\circ$  factor in the present investigations was exclusively governed by electronic energy difference. The encroaching feature of the present investigations is that both  $H_2\text{-}$  and  $Zn\text{-Pc}$  could not serve as good discriminators between  $C_{60}$  and  $C_{70}$ , as revealed from  $K$  values of the  $H_2\text{-}$  and  $Zn\text{-Pc}$  complexes of  $C_{60}$  and  $C_{70}$  (see Table 3). This phenomenon stimulated us to look into detail regarding orientation pattern of  $C_{70}$  toward the plane of phthalocyanines. We anticipated that the contact area of phthalocyanines with  $C_{60}$  would not differ much with respect to that of  $C_{70}$ . Estimation of the surface area of the  $C_{70}$  complexes of  $H_2\text{-Pc}$  (side-on),  $H_2\text{-Pc}$  (end-on),  $Zn\text{-Pc}$  (side-on) and  $Zn\text{-Pc}$  (end-on) were estimated to be 968.05, 967.84, 961.38 and 962.80 ( $\text{\AA}^2$ ), respectively. Thus, unlike fullerene/porphyrin

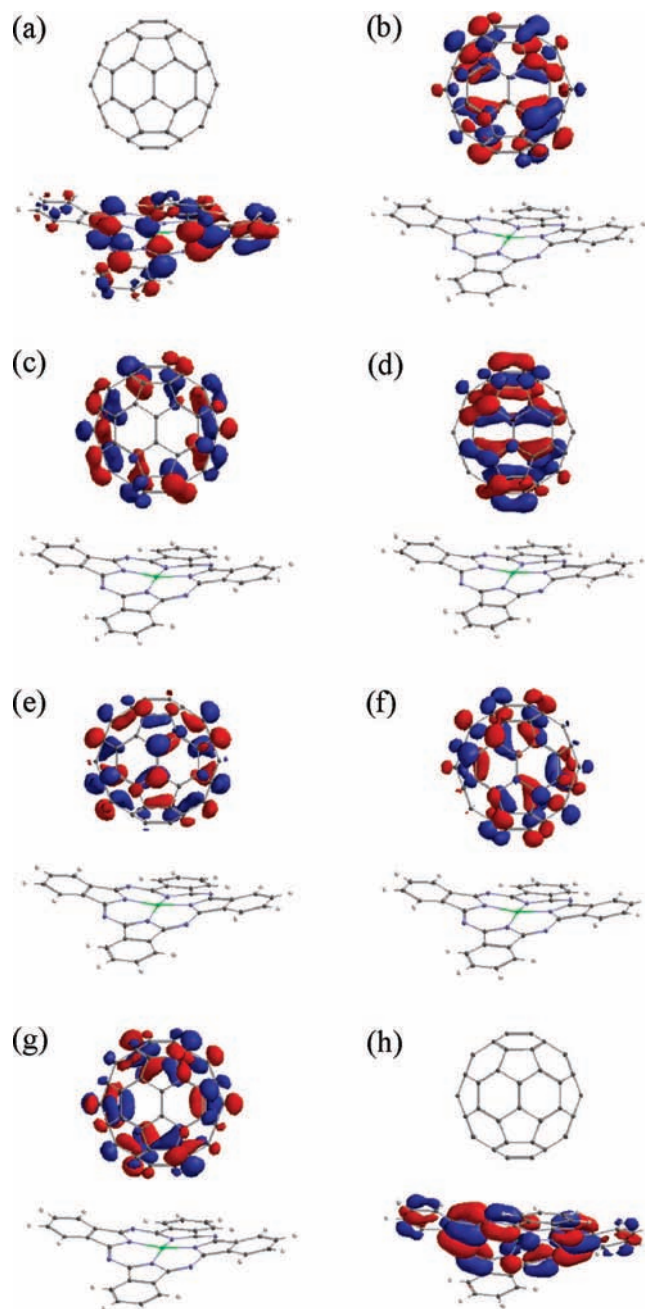


**Figure 17.** HOMOs and LUMOs of  $C_{60}/Zn\text{-Pc}$  complex at different electronic states: (a) HOMO, (b) HOMO-1, (c) HOMO-2, (d) HOMO-3, (e) LUMO, (f) LUMO+1, (g) LUMO+2 and (h) LUMO+3 done by DFT/B3LYP/6-31G\* calculations.

interaction,<sup>49,50</sup> computations of the preferred conformations of fullerene/phthalocyanine complexes confirm that van der Waals attractive forces is very much negligible for the investigated supramolecules. Figures 7–9 showed the space filling models for the phthalocyanine complexes of  $C_{60}$ ,  $C_{70}$  in side-on orientation and  $C_{70}$  in end-on orientations, respectively, and Figure 10 demonstrated the stereoscopic structures of all the fullerene/phthalocyanine complexes obtained by DFT method. Table 3 nicely demonstrated that trend in the  $\Delta H_f^\circ$  values for various fullerene/phthalocyanine complexes track superbly well with the experimentally determined binding constants. From Table 3, it is quite clear that although complex formation is enthalpy favored, it is also entropy disfavored. Formation of the complexes therefore results in a more ordered state, possibly due to the freezing of the motional freedom of both the fullerene

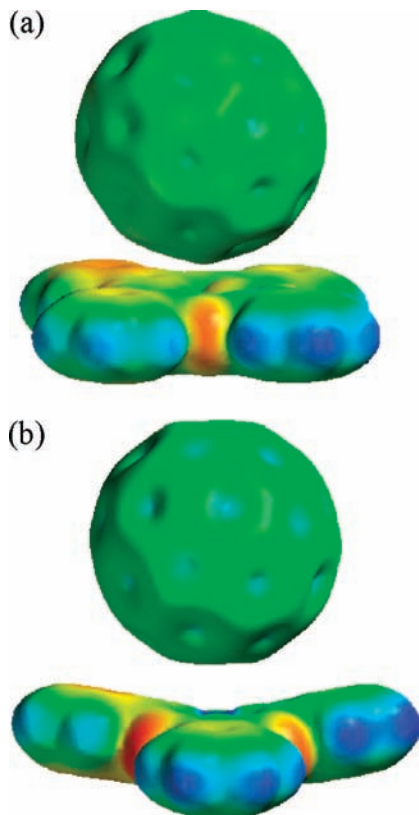


**Figure 18.** MESP plots for the  $C_{60}$  complexes of (a)  $H_2$ - and (b) Zn-Pc done by HF/3-21G calculations.

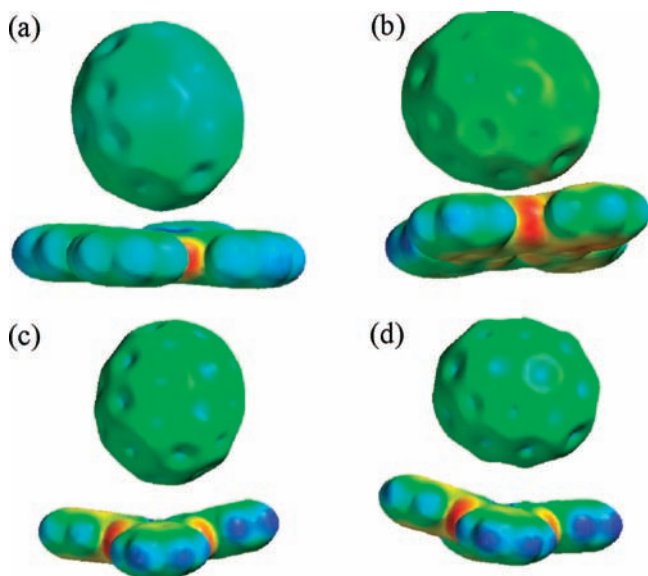


**Figure 19.** MESP plots for the  $C_{70}$  complexes of (a)  $H_2$ -Pc (end-on orientation of  $C_{70}$ ), (b)  $H_2$ -Pc (side-on orientation of  $C_{70}$ ), (c) Zn-Pc (end-on orientation of  $C_{70}$ ) and (d) Zn-Pc (side-on orientation of  $C_{70}$ ) done by HF/3-21G calculations.

and phthalocyanine molecules. Because the formation of such ensembles involves either entropically or enthalpically driven organization of individual components, the yields of the complexes frequently exceed those obtained for analogous covalent systems. Table 3 surmised that the results obtained from ab initio and DFT calculations contradicted somewhat regarding orientation behavior of  $C_{70}$  molecule toward the plane of phthalocyanines in terms of  $\Delta H_f^\circ$  value. Thus, it is observed that although the alignment of  $C_{70}$  with the plane of  $H_2$ -Pc was

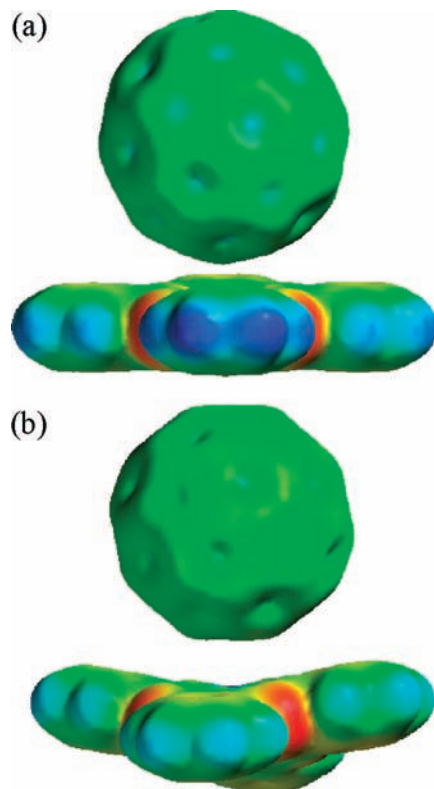


**Figure 20.** MESP plots for the  $C_{60}$  complexes of (a)  $H_2$ - and (b) Zn-Pc done by DFT/B3LYP/6-31G\* calculations.

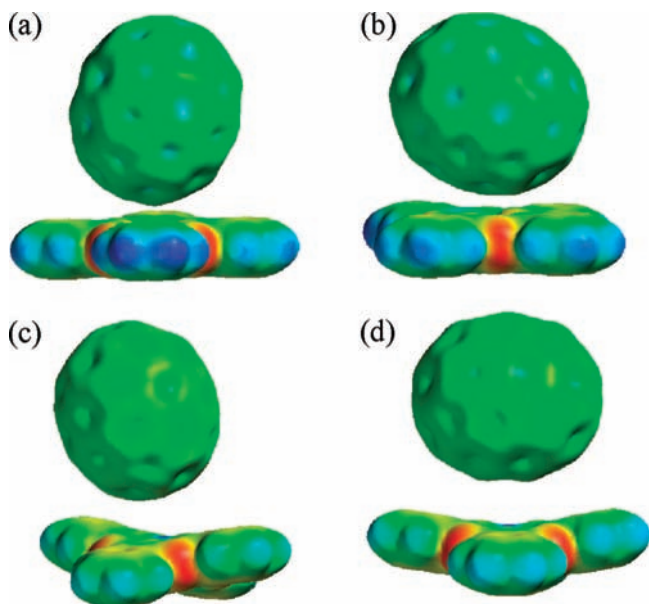


**Figure 21.** MESP plots for the  $C_{70}$  complexes of (a)  $H_2$ -Pc (end-on orientation of  $C_{70}$ ), (b)  $H_2$ -Pc (side-on orientation of  $C_{70}$ ), (c) Zn-Pc (end-on orientation of  $C_{70}$ ) and (d) Zn-Pc (side-on orientation of  $C_{70}$ ) done by DFT/B3LYP/6-31G\* calculations.

favored in end-on orientation as revealed by DFT calculation, ab initio estimated data were shown to exhibit the reverse trend. Similarly, although ab initio calculations predicted end-on approach of  $C_{70}$  toward Zn-Pc, DFT calculations follow the opposite trend. Thus, a possible criticism of the present study is that these computations were all done in vacuo, i.e., excluding the solvent. In addition to the fact that the already lengthy computations would have become even more involved if solvent were included, the decision to explicitly exclude the solvent

can be justified as the topology of these supramolecules is not sensitive to the solvent polarity.

Considering all these facts, it is very much essential to determine the binding motif of  $C_{70}$  toward phthalocyanines by some more sophisticated quantum mechanical calculation. For this reason, we have performed hybrid HF-DFT SCF calculation using Pulay DIIS and geometry direct minimization technique. We have opted to use the hybrid functional over Hartree-Fock (HF) method, as it can account for correlation effects also. Although HF describes exchange exactly, it results in unbound LUMO states. In the present calculation, good descriptions of the LUMO states are very important, as the incoming electrons are assumed to pass through it. Therefore, the use of hybrid functional in DFT formalism is fully justified. Several successful applications using hybrid functionals have been reported.<sup>51,52</sup>  $\Delta H_f^\circ$  value of  $C_{70}/H_2$ -Pc complex in side-on orientation is  $-0.576 \text{ kcal}\cdot\text{mol}^{-1}$ , which signifies that the complex is enthalpically less stable than that observed in end-on orientation, i.e.,  $-0.797 \text{ kcal}\cdot\text{mol}^{-1}$  (Figure 11). Similarly, the  $C_{70}$  complex of Zn-Pc gained  $0.58 \text{ kcal}\cdot\text{mol}^{-1}$  of enthalpy of stabilization when it oriented in an end-on manner as  $\Delta H_f^\circ C_{70}/\text{Zn-Pc}(\text{end-on}) = 5.55 \text{ kcal}\cdot\text{mol}^{-1}$  and  $\Delta H_f^\circ C_{70}/\text{Zn-Pc}(\text{side-on}) = 6.13 \text{ kcal}\cdot\text{mol}^{-1}$  (Figure 12).

The above results proclaim that the supramolecular binding pattern of both  $C_{60}$  and  $C_{70}$  were almost similar toward phthalocyanines. Evidence in favor of end-on orientation of  $C_{70}$  toward the plane of the phthalocyanines, got strong experimental support from  $^{13}\text{C}$  NMR experiment of  $C_{70}/\text{Zn-Pc}$  system recorded in toluene- $d_8$  medium (Figure 13). It was already reported that chemical shifts of free  $C_{70}$  appear at 151.07, 147.52, 146.82, 144.77 and 131.0, due to existence of five different type of carbon atoms, namely, polar,  $\alpha$ ,  $\beta$ ,  $\gamma$  and equatorial, respectively.<sup>53-55</sup> In our present investigation, it has been observed that although the equatorial peak has got only 0.5 ppm perturbation in terms of difference in chemical shift value, the peak at the pole region suffers a considerable amount of ion in terms of chemical shift value, i.e., 4.2 ppm. This phenomenon clearly demonstrates that the pole region of  $C_{70}$  approaches closely toward the plane of the phthalocyanine, resulting in an end-on orientation of such molecule. Thus, the approaching surface area of both  $C_{60}$  and  $C_{70}$  toward the plane of  $H_2$ - and Zn-Pc remain almost the same, which was reflected in binding constant values of such complexes. Both theoretical and experimental observations envisaged that such a binding motif of  $C_{70}$  toward phthalocyanines took place to maximize the electrostatic interactions. This feature envisages that, unlike  $C_{70}/\text{porphyrin}$  interaction,<sup>56,57</sup> the presence of dispersive forces associated with  $\pi$ - $\pi$  interactions were very much negligible in present case. However, it should be noted at this point that  $\Delta H_f^\circ$  values determined by DFT calculations for the fullerene/phthalocyanine complexes give much more reliable data, as  $\text{C-H}\cdots\pi$  interactions are generally not counted in the ab initio calculations.

Considering all these facts and to gain substantial information on molecular and electronic structure of the fullerene/phthalocyanine complexes, computational studies were performed in explicit manner using DFT calculations at the B3LYP/6-31G\* level. The optimized structures of the fullerene/phthalocyanine complexes reveal closely spaced phthalocyanine and  $C_{70}$  entities in comparison to  $C_{60}$  (Figure 10). Stereoscopic structures of various fullerene/phthalocyanine complexes depicted in Figure 10 clearly validate that the equatorial region of  $C_{70}$  was unable to cover all the  $\pi$ -electron rich surface area of phthalocyanines. On the contrary, the pole region of  $C_{70}$  directly approaches

toward the inner core of phthalocyanines in such a manner that we could not identify the perturbation in electron density between 6:5 (pole region) and 6:6 (equatorial region) ring-juncture of  $C_{70}$ . For the  $C_{60}/\text{Zn-Pc}$  complex, the average Zn-N distance of the axial coordination bond was computed to be 1.944 and 1.939 Å, in ab initio and DFT calculations, respectively, which was very similar to the case of the  $C_{70}/\text{Zn-Pc}$  complex. It was also observed that the Zn metal was pulled out of the phthalocyanine plane after complex formation with fullerenes. The  $\angle\text{N1-Zn1-N2}$  and  $\angle\text{N3-Zn1-N4}$  dihedral angles in the case of the  $C_{60}/\text{Zn-Pc}$  complex were computed to be  $167.85^\circ$  and  $167.93^\circ$ , respectively. DFT calculations validate the results obtained in the ab initio calculations. However, in the case of the  $C_{70}/\text{Zn-Pc}$  complex (both end-on and side-on orientations of  $C_{70}$ ), although reduction in dihedral angles took place in the case of  $\angle\text{N1-Zn1-N2}$ , viz.,  $167.79^\circ$ , a  $0.11^\circ$  increase was observed in the case of  $\angle\text{N3-Zn1-N4}$  in both ab initio and DFT levels of theory. The larger center-to-center distance in the case of  $C_{60}$  and phthalocyanine was due to weaker interaction between the phthalocyanine and fullerene, which was reflected in the trend of the  $K$  values in Table 3, i.e.,  $K_{C70} > K_{C60}$ .

The above structural analysis indicates that, unlike porphyrin, phthalocyanine and fullerene  $\pi$ -electrons in the presently investigated fullerene/phthalocyanine complexes would not strongly interact owing to their distant proximity.

In our present investigations, the existence of the electrostatic interactions between the phthalocyanine macrocycle and fullerene moiety was also evidenced by the results obtained on frontier highest occupied molecular orbital (HOMO) and lowest unoccupied molecular orbital (LUMO) using HF/3-21G method. The position of the HOMO on the phthalocyanine moiety certainly indicates that they act as donor molecules during formation of complexes with fullerenes. However, the majority of the orbital distributions of HOMO at higher excited state, viz., HOMO-1, HOMO-2 and HOMO-3 were found to be located on fullerene moiety. On the other hand, all the orbital distributions of the LUMO were positioned in fullerene entity (except LUMO + 3). This is a clear indication that CT interactions took place between fullerene and phthalocyanine in the ground state. Some pictures of HOMOs and LUMOs of the  $C_{60}$  complexes of  $H_2$ - and Zn-Pc are visualized in Figures 14 and 15, respectively. The  $C_{70}$  complexes of  $H_2$ - and Zn-Pc are shown in Figures 6S-9S, Supporting Information, respectively. The present findings accord superbly with our previous findings obtained from UV-vis experiments as discussed above. Energies of HOMO ( $E_{\text{HOMO}}$ ) and LUMO ( $E_{\text{LUMO}}$ ) of all the fullerene complexes along with the individual components are given in Tables 4 and 5. So, it is also very essential to determine the position of HOMOs and LUMOs precisely, as they govern the CT phenomena. Although existence of HOMOs and LUMOs at various electronic states done by DFT calculations corroborate fairly well with those reported by ab initio calculations, the HOMO-LUMO gap is much lower in the former case compared to the latter. Moreover, the HOMO-LUMO energy gap of the  $C_{70}/\text{phthalocyanine}$  complexes corroborate excellently with the reported CT transition energies of same complexes. In our present investigations, the HOMO-LUMO energy gap of the  $C_{70}$  complexes of  $H_2$ - and Zn-Pc were estimated to be 628 and 690 nm, respectively, which agree fairly well with the experimentally determined values of CT transition energies of same systems, i.e., 694 and 702 nm, respectively. Thus, DFT calculation provides a rational support in favor of our experimentally obtained CT absorption band. However, in the case

of C<sub>60</sub> complexes, there is a considerable variation between the experimentally reported and theoretically determined values of CT transition energy. This is because DFT calculations were done in vacuo, which did not consider the effect of solvent. Typical pictorial representations containing HOMO and LUMO of the C<sub>60</sub> complexes of both H<sub>2</sub>- and Zn-Pc, done by DFT calculations at various electronic states are shown in Figures 16 and 17, respectively. HOMOs and LUMOs of the C<sub>70</sub>/H<sub>2</sub>-Pc and C<sub>70</sub>/Zn-Pc complexes in end-on and side-on orientations of C<sub>70</sub> are provided as Figures 10S–13S, Supporting Information. Energies of various HOMOs and LUMOs of the fullerene complexes of phthalocyanines along with uncomplexed fullerenes and phthalocyanines at DFT/B3LYP/6-31G\* levels of theory are given in Tables 6 and 7.

Moreover, molecular electrostatic potential (MESP) map calculation by the ab initio method reveals that the regions of high negative electrostatic potential of the phthalocyanine (the four N atoms) were facing the regions of strong positive electrostatic potential of the fullerenes (the centers of hexagons and pentagons) and vice versa (6:6 bond is high negative electrostatic potential and Zn is high positive electrostatic potential) (Figures 18 and 19). The same reasoning can be done in terms of high charge density and low regions. DFT calculations (Figures 20 and 21) establish the results obtained in HF calculations. However, the complex structure of C<sub>70</sub> with H<sub>2</sub>- and Zn-Pc (see Figure 21) reveals that the distribution of electronic potentials over the surface area of both the donor (phthalocyanines) and acceptor (fullerenes) molecules of fullerene/phthalocyanine complexes took place in such a manner that electrostatic interactions play dominant role behind the mode of approach of C<sub>70</sub> toward the plane of the phthalocyanines. Therefore, in these particular systems, the electrostatic interaction eventually determined the absorption geometry of the phthalocyanine (Figures 14S and 15S, Supporting Information) with respect to fullerenes (Figures 16S and 17S, Supporting Information).

#### 4. Conclusion

After summarizing the results of the present investigations, we reach the following conclusions:

(1) Both H<sub>2</sub>- and Zn-Pc undergo ground state CT interaction with fullerenes C<sub>60</sub> and C<sub>70</sub>; degrees of CT indicate that low percentage of charge transfer takes place in the ground state.

(2) For the first time, the present investigation reports the experimentally determined vertical ionization potential values of both free-base and metallo-phthalocyanines in solution phase.

(3) Binding constants of the fullerene/phthalocyanine complexes were estimated from the fluorescence quenching experiment; the increase in magnitude of binding constant led to increase in the fluorescence quenching efficiency.

(4) Magnitude of *K* values of the fullerene complexes of H<sub>2</sub>- and Zn-Pc suggests that both the phthalocyanines were unable to discriminate between C<sub>60</sub> and C<sub>70</sub>. The above finding proves that these two phthalocyanines could not be effectively employed for the extraction of fullerenes in solution.

(5) Hybrid HF-DFT calculations suggest that orientation of C<sub>70</sub> toward the plane of H<sub>2</sub>- and Zn-Pc is end-on rather than side-on which proves that dispersive forces associated with  $\pi$ – $\pi$  interactions are not the key factor behind the effective fullerene/phthalocyanine complexation. <sup>13</sup>C NMR experiment provides very good support in favor of theoretical calculation regarding binding pattern of C<sub>70</sub> toward phthalocyanines.

(6) Observation of CT spectra between fullerene and phthalocyanine can be understood in terms of HOMO–LUMO

interactions. Molecular electrostatic potential map calculations clearly demonstrate that charge transfer took place in the ground state from phthalocyanine to fullerene.

(7) Finally, we can say that the results emanating from present investigations could be of potential interest in studying the photoinduced energy and electron transfer phenomena of fullerene/phthalocyanine model system in near future.

**Acknowledgment.** A.R. acknowledges The University of Burdwan for providing her junior research fellowship through state funded project. This work is financially supported by Department of Science and Technology, New Delhi, India, through Fast Track scheme of Sanction No. SR/FTP/CS-22/2007. We record our gratitude to the Editor of *The Journal of Physical Chemistry* and the learned reviewers for making valuable comments.

**Supporting Information Available:** UV–vis absorption spectra of only H<sub>2</sub>-Pc in toluene along with mixture H<sub>2</sub>-Pc with C<sub>60</sub>, C<sub>70</sub>, TCNE, TCNQ and *p*-chloranil, variation of  $\alpha$  with electron affinity for H<sub>2</sub>-Pc and Zn-Pc, plots of fluorescence intensity versus emission wavelength for the C<sub>70</sub> complexes of H<sub>2</sub>-Pc and Zn-Pc, plots of relative fluorescence intensity vs concentration of C<sub>70</sub> for the C<sub>70</sub> complexes of H<sub>2</sub>-Pc and Zn-Pc, BH fluorescence plots of the C<sub>70</sub>/H<sub>2</sub>-Pc and C<sub>60</sub>/Zn-Pc systems in toluene medium, HOMOs and LUMOs of C<sub>70</sub> complexes of both H<sub>2</sub>-Pc and Zn-Pc in different orientations of C<sub>70</sub> done by HF/3-21G and DFT/B3LYP/6-31G\* calculations along with MESP of H<sub>2</sub>-Pc, Zn-Pc, C<sub>60</sub> and C<sub>70</sub> obtained by both HF/3-21G and DFT/B3LYP/6-31G\* calculations are given as Figures 1S–17S, respectively. This material is available free of charge via the Internet at <http://pubs.acs.org>.

#### References and Notes

- (1) Lehn, J.-M. *Supramolecular Chemistry: Concepts and perspectives*; VCH: Weinheim, 1995.
- (2) Sessler, J. L.; Wang, B.; Springs, S. L.; Brown, C. T. *Comprehensive Supramolecular Chemistry*; Pergamon Press: Oxford, 1996.
- (3) Balzani, V.; Credi, A.; Raymo, F. M.; Stoddart, J. F. *Angew. Chem., Int. Ed.* **2000**, *39*, 3348.
- (4) (a) *Phthalocyanines: Properties and Applications*; Leznoff, C. C., Lever, A. B. P., Eds.; VCH: Weinheim, 1989, 1993, 1996; Vols. 1–4. (b) Torre, de la G.; Nicolan, M.; Torres, T. In *Phthalocyanines: Synthesis, Supramolecular Organization and Physical Properties (Supramolecular Photosensitive and Electroactive Materials)*; Nalwa, H. S., Ed.; Academic Press: New York, 2001.
- (5) Tanaka, D.; Rikukawa, M.; Sanui, K.; Ogata, N. *Synth. Met.* **1999**, *102*, 1492.
- (6) Fujiki, M.; Tabei, H.; Kurihara, T. *J. Phys. Chem.* **1988**, *92*, 1281.
- (7) Subbiah, S.; Mokaya, R. *J. Phys. Chem. B* **2005**, *109*, 5079.
- (8) Van Nostrum, C. F.; Nolte, R. J. M. *Chem. Commun.* **1996**, 2385.
- (9) Hirsch, A., Ed. *Fullerenes and Related Structures*; Springer: Berlin, 1999; Vol 1999.
- (10) Iglesias, R. S.; Claessens, C. G.; Torres, T.; Rahman, G. M. A.; Guldi, D. M. *Chem. Commun.* **2005**, 2113.
- (11) Gouloumis, A.; Liu, S.-G.; Sastre, A.; Vázquez, P.; Echegoyen, L.; Torres, T. *Chem. Eur. J.* **2000**, *6*, 3600.
- (12) González-Rodríguez, D.; Torres, T.; Herranz, M. A.; Rivera, J.; Echegoyen, L.; Guldi, D. M. *J. Am. Chem. Soc.* **2004**, *126*, 6301.
- (13) Ballesteros, B.; de la Torre, G.; Torres, T.; Hug, G. L.; Rahman, G. M. A.; Guldi, D. M. *Tetrahedron* **2006**, *62*, 2097.
- (14) de la Escosura, A.; Martínez-Díaz, M. V.; Guldi, D. M.; Torres, T. *J. Am. Chem. Soc.* **2006**, *128*, 4112.
- (15) Rispen, M. T.; Sánchez, L.; Knol, J.; Hummelen, J. C. *Chem. Commun.* **2001**, 161.
- (16) Torres, T.; Gouloumis, A.; Sanchez-Garcia, D.; Jayawickramarajah, J.; Seitz, W.; Guldi, D. M.; Sessler, L. J. *Chem. Commun.* **2007**, 292.
- (17) Koeppel, R.; Troshin, P. A.; Fuchsbaue, A.; Lyubovskaya, R. N.; Sariciftci, N. S. *Fullerenes, Nanotubes Carbon Nanostruct* **2006**, *14*, 441.
- (18) Guldi, D. M.; Gouloumis, A.; Vanquez, P.; Torres, T. *Chem. Commun.* **2002**, 2056.
- (19) Zhu, P. W.; Wang, P.; Qiu, W.; Liu, Y.; Ye, C.; Fang, G.; Song, Y. *Appl. Phys. Lett.* **78** **2001**, 1319.

- (20) Zhan, H. B.; Chen, W. Z.; Yu, H.; Wang, M. Q. *J. Mater. Lett.* **2003**, *57*, 1361.
- (21) Venturini, J.; Kououmas, E.; Couris, S.; Janot, J. M.; Seta, P.; Mathis, C.; Leach, S. *J. Mater. Chem.* **2002**, *12*, 2071.
- (22) Bhattacharya, S.; Shimawaki, T.; Peng, X.; Ashokkumar, A.; Aonuma, S.; Kimura, T.; Komatsu, N. *Chem. Phys. Lett.* **2006**, *430*, 435.
- (23) Bhattacharya, S.; Nayak, S. K.; Chattopadhyay, S.; Ghosh, K.; Banerjee, M. *Spectrochim. Acta Part A* **2007**, *67*, 1257.
- (24) Martinez-Diaz, M. V.; Fenderm, N. S.; Rodriguez-Morgade, M. S.; Lo'pez, M. G.; Diederich, F.; Echegoyen, L.; Stoddart, J. F.; Torres, T. *J. Mater. Chem.* **2002**, *12*, 2095.
- (25) Mulliken, R. S. *J. Am. Chem. Soc.* **1952**, *74*, 811.
- (26) Bhattacharya, S.; Nayak, S. K.; Chattopadhyay, S.; Banerjee, M.; Mukherjee, A. K. *Spectrochim. Acta Part A* **2002**, *58*, 289.
- (27) Bhattacharya, S.; Banerjee, M.; Mukherjee, A. K. *Spectrochim. Acta Part A* **2001**, *57*, 1463.
- (28) (a) R. Foster, *Organic Charge Transfer Complexes*; Academic Press: New York, 1969; Chapters 3 and 13. (b) Peover, M. E. *J. Chem. Soc.* **1962**, 4540.
- (29) Peover, M. E. *J. Chem. Soc.* **1962**, 4540.
- (30) Bhattacharya, S.; Banerjee, M.; Mukherjee, A. K. *Spectrochim. Acta Part A* **2001**, *57*, 2409.
- (31) Guldi, D.; Gouloumis, A.; Va'zquez, P.; Torres, T. *Chem. Commun.* **2002**, 2056.
- (32) Antonietta Loi, M.; et al. *J. Mater. Chem.* **2003**, *13*, 700.
- (33) Ito, O.; D'Souza, F. *Coord. Chem. Rev.* **2005**, *249*, 1410.
- (34) Yin, G.; Xu, D.; Xu, Z. *Chem. Phys. Lett.* **2002**, *365*, 232.
- (35) Armaroli, N. *Photochem. Photobiol. Sci.* **2003**, *2*, 73.
- (36) Armaroli, N.; Marconi, G.; Echegoyen, L.; Bourgeois, J.-P.; Diederich, F. *Chem.-A Eur. J.* **2000**, *6*, 1629.
- (37) Benesi, H. A.; Hildebrand, J. H. *J. Am. Chem. Soc.* **1949**, *71*, 2703.
- (38) Yin, G.; Xu, D.; Xu, Z. *Chem. Phys. Lett.* **2002**, *365*, 232.
- (39) Guldi, D. M.; Da Ros, T.; Braiuca, P.; Prato, M. *Photochem. Photobiol. Sci.* **2003**, *2*, 1067.
- (40) Bhattacharya, S.; Tominaga, K.; Kimura, T.; Uno, H.; Komatsu, N. *Chem. Phys. Lett.* **2007**, *433*, 395.
- (41) Bhattacharya, S.; Komatsu, N.; Banerjee, M. *Chem. Phys. Lett.* **2005**, *406*, 509.
- (42) Wang, M.-X.; Zhang, X.-H.; Zheng, Q.-Y. *Angew. Chem., Int. Ed.* **2004**, *43*, 838.
- (43) Dudič, M.; Lhot'ak, P.; Stibor, I.; Petříčkov'a, H.; Lang, K. *New J. Chem.* **2004**, *28*, 85.
- (44) Shoji, Y.; Tashiro, K.; Aida, T. *J. Am. Chem. Soc.* **2004**, *126*, 6570.
- (45) Mustafizur Rahman, A. F. M.; Bhattacharya, S.; Peng, X.; Kimura, T.; Komatsu, N. *Chem. Commun.* **2008**, 1196.
- (46) Mizyed, S.; Tremaine, P. R.; Georghiou, P. E. *J. Chem. Soc., Perkin Trans. 2* **2001**, 3.
- (47) Haino, T.; Yanase, M.; Fukuzawa, Y. *Angew. Chem., Int. Ed. Engl.* **1997**, *36*, 259.
- (48) Zhou, X.; Gu, Z.; Wu, Y.; Sun, Y.; Jin, Z.; Xiong, Y.; Sun, B.; Wu, Y.; Fu, H.; Wang, J. *Carbon* **1994**, *32*, 935.
- (49) Boyd, P. D. W.; Reed, C. A. *Acc. Chem. Res.* **2005**, *38*, 235.
- (50) Sun, D. Y.; Tham, F. S.; Reed, C. A.; Chaker, L.; Boyd, P. D. W. *J. Am. Chem. Soc.* **2002**, *124*, 6604.
- (51) Salzner, U. *Synth. Met.* **1999**, *101*, 482.
- (52) Seminario, J. M.; Zacarias, A. G.; Tour, J. M. *J. Am. Chem. Soc.* **2000**, *122*, 3015.
- (53) Taylor, R. *Lecture Notes on Fullerene Chemistry: A Handbook for Chemist*; Imperial Press: London, 1999.
- (54) Hanna, J. V.; Wilson, M. A. *J. Phys. Chem.* **1992**, *96*, 6518.
- (55) Taylor, R.; Hare, J. P.; Abdul-Sada, A. K.; Kroto, H. W. *Chem. Commun.* **1990**, 1423.
- (56) Lee, K.; Song, H.; Park, J. T. *Acc. Chem. Res.* **2003**, *36*, 78.
- (57) Bhattacharya, S.; Nayak, S. K.; Chattopadhyay, S.; Ghosh, K.; Banerjee, M. *Spectrochim. Acta Part A* **2007**, *67*, 1257.

JP807123V